Proc. Natl. Acad. Sci. USA
Vol. 85, pp. 6122–6126, August 1988
Medical Sciences

Unusual lipid structures selectively reduce the toxicity of amphotericin B

(liposomes/polyene antibiotics/antifungal agents/membrane morphology)

A. S. JANOFF*†, L. T. BONI*, M. C. POPESCU*, S. R. MINCHEY*, P. R. CULLIS‡, T. D. MADDEN‡§, T. TARASCHI§¶, S. M. GRUNER‖, E. SHYAMSUNDER‖, M. W. TATE‖, R. MENDELSOHN**, AND D. BONNER††

*The Liposome Company, Inc., 1 Research Way, Princeton, NJ 08540; ‡Department of Biochemistry, University of British Columbia, 2146 Health Sciences Mall, Vancouver, BC, Canada V6T 1W5; ¶Department of Pathology, Thomas Jefferson University, Foerderer Pavillion, 11th and Walnut Streets, Philadelphia, PA 19107; ‖Department of Physics, Princeton University, P.O. Box 708, Princeton, NJ 08540; **Department of Chemistry, Rutgers University, 73 Warren Street, Newark, NJ 07102; and ††The Squibb Institute for Medical Research, P.O. Box 4000, Princeton, NJ 08540

Communicated by Bengt Samuelsson, April 15, 1988 (received for review December 18, 1987)

ABSTRACT **Ribbon-like structures result when amphotericin B interacts with lipid in an aqueous environment. At high ratios of amphotericin to lipid these structures, which are lipid-stabilized amphotericin aggregates, become prevalent resulting in a dramatic attenuation of amphotericin-mediated mammalian cell, but not fungal cell, toxicity. Studies utilizing freeze–etch electron microscopy, differential scanning calorimetry, ^{31}P NMR, x-ray diffraction, and optical spectroscopy revealed that this toxicity attenuation is related to the macromolecular structure of the complexes in a definable fashion. It is likely that amphotericin in this specific form will have a much improved therapeutic utility.**

Amphotericin B, a polyene antibiotic, is the drug of choice for a variety of systemic fungal infections that were almost always fatal prior to its introduction (1). The cytotoxic mechanism of this compound has been the subject of intensive investigation over many years and is thought to reside in its ability to form membrane ion channels particularly in the presence of sterols (2). That these channels and associated lethal permeability changes occur at somewhat lower membrane concentrations in the presence of ergosterol (the predominant sterol in fungal cell membranes) rather than cholesterol (the predominant sterol in mammalian cell membranes) most likely forms the basis of the selective toxicity of this drug (3). Still, in its present dosage form, which is a deoxycholate micelle, its clinical utility is profoundly limited by host cell toxicity particularly in those cases (such as in patients with acquired immunodeficiency syndrome) where high-dose therapy is indicated.

Much attention has focused on liposome suspensions containing 5–10 mol % amphotericin B because these systems have been shown to produce a significant attenuation of toxicity with little compromise to efficacy (4–7). In fact one such formulation in which amphotericin comprises 5 mol % of a 1,2-dimyristoyl-*sn*-glycero(3)phosphocholine/1,2-dimyristoyl-*sn*-glycero(3)phospho(1)-*rac*-glycerol ([Myr_2]PtdCho/[Myr_2]PtdGro) suspension, 7:3 (mol/mol), has shown great promise in human clinical trials (8, 9). Unfortunately, the mechanistic foundations allowing this promise have remained obscure despite attempts to elucidate them. For instance, suggestions that altered tissue distributions might play a primary role have been confounded by direct pharmacodynamic measurements (10) and demonstrations that similar toxicity attenuations can occur *in vitro* (11). Although it now seems clear that fundamentally molecular phenomena must be involved, there currently exists no simple testable biophysical model to explain why the interaction of amphotericin B with mammalian cell receptors would be altered by incorporation of the drug in a liposomal rather than micellar dispersion. Our work in this area, which focuses on the clinically relevant [Myr_2]PtdCho/[Myr_2]PtdGro, 7:3 (mol/mol), formulation, has addressed this issue. Here we report that when these lipids are combined with amphotericin and hydrated fully, structures clearly distinct from liposomes result. These structures are apparently responsible for the enhanced selective toxicity that has been widely reported to result from the incorporation of this drug into intact vesicles.

MATERIALS AND METHODS

Sample Preparation. Samples were prepared following the multilamellar vesicle procedure. Typically between 73 and 142 mg of [Myr_2]PtdCho/[Myr_2]PtdGro at a molar ratio of 7:3 was deposited from chloroform as a thin film on the bottom of a 500-ml round-bottomed flask by rotoevaporation. This film was solubilized in 100 ml of amphotericin B in methanol (0.1 mg/ml) and again rotoevaporated to a thin film. When dry, the film was suspended in isotonic phosphate-buffered saline (PBS) and subjected to bath sonication for 0.5 hr or until particles exhibiting Brownian motion were observed by phase-contrast microscopy.

Sucrose Density Centrifugation. Typically, 200 μl of material was layered onto a continuous sucrose gradient in 150 mM NaCl/20 mM Hepes, pH 7.4. The gradient was centrifuged for 22 hr at 22°C in a SW 60 rotor (Beckman) at 230,000 $\times$ *g*. After centrifugation the gradient was fractionated into 150-μl aliquots and assayed for amphotericin B (from absorbance at 412 nm in dimethylformamide) and phospholipid (from phosphate assay after digestion).

***In Vivo* Toxicity.** LD_{50} values were determined by the method of Reed and Muench (12). Female Swiss Webster mice (22–24 g) received 0.5 ml of material by intravenous injections, and lethality was registered for 10 days. A total of six mice were used at each dosage level.

***In Vitro* Toxicity.** The concentration of samples necessary to produce 10% hemolysis (H_{10}) in a 4% (vol/vol) washed erythrocyte suspension in PBS was determined so that *in vitro* toxicities could be assessed. Hemolysis was determined spectrophotometrically at 550 nm after sample incubation for 20 hr at 37°C and low-speed centrifugation. One hundred percent hemolysis was effected by a 1:1 dilution with distilled water.

Abbreviations: [Myr_2]PtdCho, 1,2-dimyristoyl-*sn*-glycero(3)phosphocholine; [Myr_2]PtdGro, 1,2-dimyristoyl-*sn*-glycero(3)phospho(1)-*rac*-glycerol.

†To whom reprint requests should be addressed.
§Present address: The Canadian Liposome Co., Ltd., 267 West Esplanade, Suite 308, North Vancouver, BC, Canada V7M 1A5.

The publication costs of this article were defrayed in part by page charge payment. This article must therefore be hereby marked "*advertisement*" in accordance with 18 U.S.C. §1734 solely to indicate this fact.

Efficacy. Efficacy was based on 21-day survival studies. Swiss Webster female mice (five per group) were infected i.v. with 0.2 ml of a *Candida albicans* suspension (SG 5314) in saline (determined microscopically to contain 2.5×10^7 cells per ml). Five hours after inoculation, the animals were treated with either 0.2 ml of a lipid dispersion containing 50 mol % amphotericin or amphotericin solubilized in deoxycholate micelles.

Freeze–Etch Electron Microscopy. Samples were prepared by quick freezing into liquid propane without a cryoprotectant. Typically between 0.1 and 0.3 μl of the specimen was sandwiched between a pair of copper-support plates [Balzers (Nashua, NH)] and rapidly plunged from 20°C into liquid propane. Samples were fractured and replicated on a double replicating device in a Balzers freeze–fracture unit at a vacuum of 2×10^{-6} mbar (1 bar = 10^5 Pa) or better at −115°C. Replicas were "floated off" in 3 M HNO_3 and then washed in a graded series of Clorox solutions. These were finally cleaned in distilled water and picked up on 300-Hex-mesh copper grids (Polyscience, Warrington, PA). Replicas were viewed with a Philips 300 electron microscope at a magnification of ×25,000.

Captured Volumes. Captured volumes were determined by hydrating the lipid/amphotericin B film in PBS buffer containing tracer amounts of [^{3}H]inulin (0.5 μCi/ml; 1 Ci = 37 GBq). Untrapped inulin was removed by a 1:10 dilution with unlabeled buffer subsequent to centrifugation. After the final washing step, the pellet was suspended in a minimal volume and assayed for lipid phosphorus and [^{3}H]inulin. Trapped volumes were calculated and expressed as microliters of aqueous trapped volume per micromole of phospholipid. Care was taken during the entire procedure to maintain the lipid mixture at 4°C.

Differential Scanning Calorimetry. Measurements were carried out on an MC-1 unit from Micro Cal (Amherst, MA). Sample volumes of 0.70 ml containing 17–25 mg of lipid were injected into the sample cell with the same volume of buffer used in the reference cell. Samples were heated at either 26°C per hr or 37°C per hr. Duplicate runs of the same sample with the same history gave onset and completion temperatures reproducible to 0.2°C. In some cases, samples containing amphotericin were heated to 60°C (and no higher) and then cooled to 2–4°C for at least 2 hr prior to rescanning.

^{31}P NMR. Spectra were obtained at 145.7 MHz on a Bruker AM360 wide-bore NMR spectrometer with 8000 data points for acquisition, a sweep width of 50 kHz, and a pulse width of 20 msec corresponding to a 45° pulse. Spectra were accumulated from up to 10,000 transients at 25°C.

Wide-Angle X-Ray Diffraction. X-ray diffraction measurements were performed as described (13).

Absorbance Spectroscopy. In all cases samples were placed in 1-cm path-length polymethacrylate cells and spectra were acquired at a scan rate of 100 nm/min on a Beckman model 35 spectrophotometer.

RESULTS AND DISCUSSION

Fig. 1 shows the isopycnic sucrose density profiles of three amphotericin/lipid preparations formulated so that ampho-

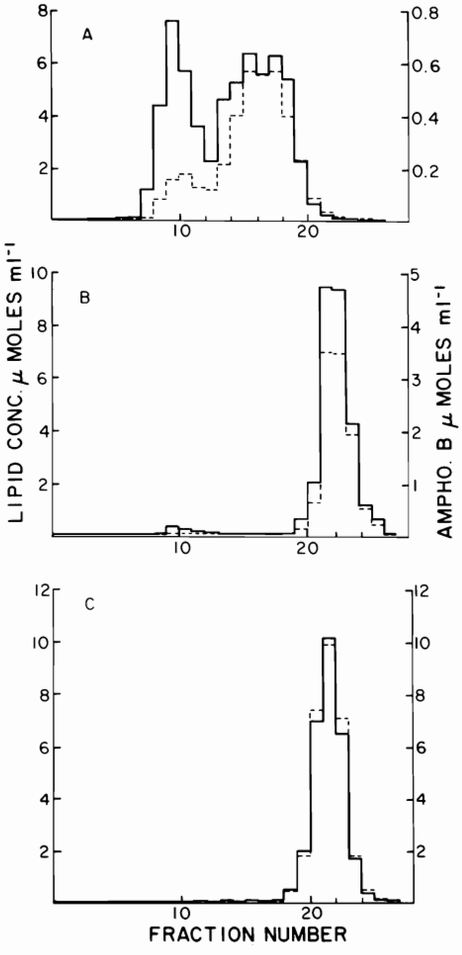

FIG. 1. Isopycnic sucrose density profiles of [Myr_2]PtdCho/[Myr_2]PtdGro, 7:3 (mol/mol), lipid dispersions incorporating 5 mol % (*A*), 25 mol % (*B*), and 50 mol % (*C*) amphotericin B. The solid lines represent lipid; the broken lines represent amphotericin. The gradient ranged from 0 to 29% (wt/wt) sucrose for the 5 and 25 mol % samples and from 0 to 41% (wt/wt) sucrose for the 50 mol % sample.

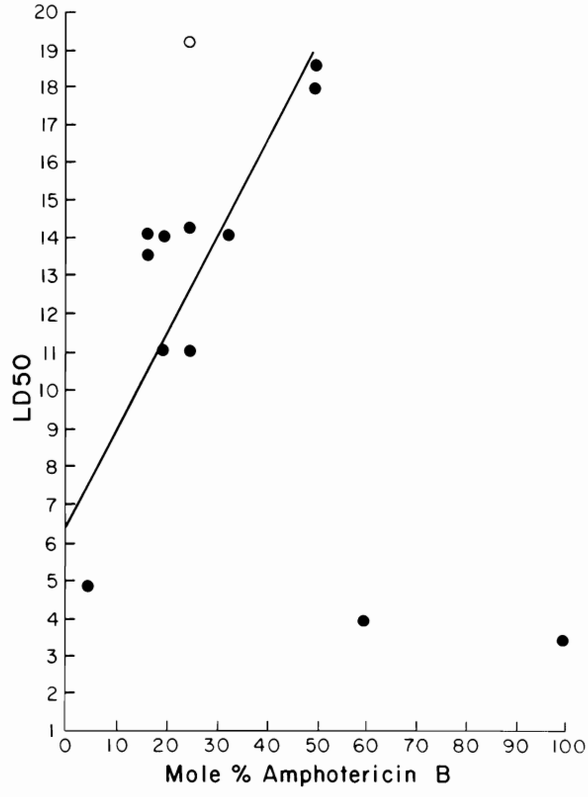

FIG. 2. Ten-day acute LD_{50} values in mice (expressed as mg of amphotericin per kg of body weight) vs. the mol % of amphotericin incorporated into [Myr_2]PtdCho/[Myr_2]PtdGro, 7:3 (mol/mol), lipid dispersions. In these experiments lipid alone was not toxic. Open circle, effect of a prior heating step on the toxicity of the 25 mol % preparation (see text).

tericin was 5, 25, or 50 mol % of the bulk lipid. The 5 mol % preparation showed a bimodal density distribution in which the bulk of the amphotericin did not migrate with the bulk of the lipid. We determined the 10-day acute toxicities of both major fractions in female Swiss Webster mice. Surprisingly, the low density lipid-enriched fraction produced an LD_{50} of 7.5 mg/kg, whereas the high-density amphotericin-enriched fraction produced an LD_{50} of 11.2 mg/kg. Thus we investigated the toxicological properties of high-mole-fraction amphotericin systems.

As shown in Fig. 1 *B* and *C*, these preparations produced density profiles in which the amphotericin was associated with >95% of the available lipid in a single band. Remarkably, elevating the mol fraction of amphotericin from 5 to 50% of the bulk lipid resulted in a dramatic decrease in toxicity as indicated in Fig. 2. When the mol fraction of amphotericin exceeded that of the lipid, however, toxicity increased to levels close to those determined for free amphotericin (100 mol %). Similar toxicity profiles were acquired in an *in vitro* hemolysis model, but efficacy as judged in an *in vivo* candidiasis model was comparatively unchanged by manipulating drug/lipid molar ratios. These experiments convinced us that to understand the underlying molecular mechanisms operating in these dispersions a more biophysical approach would be necessary.

Fig. 3 shows a series of freeze–etch electron micrographs of [Myr_2]PtdCho/[Myr_2]PtdGro, 7:3 (mol/mol), systems containing 0, 5, 25, and 50 mol % amphotericin. Lipid dispersions free of amphotericin contained numerous vesicles, some of which were many micrometers in diameter. All vesicles exhibited the P_{β}' (ripple) structure characteristic of saturated lecithins when quenched between their pre- and main transition temperatures. When 5 mol % amphotericin was incorporated into the bulk lipid, however, clumps of loosely packed ribbon structures, most likely arising from membrane systems possessing rigid hydrophobic cores, became apparent. Vesicles exhibiting the P_{β}' phase were also present but now most were <1 μm in diameter. Increasing the amphotericin content to 25 mol % resulted in a complete loss of defined liposomal structures. The predominant ribbon-like structures, on the other hand, seemed more tightly packed and clearly defined. There was no evidence of P_{β}' lipid. Qualitatively similar ribbon structures existed in the 50 mol % samples but tended to be replaced in the 60 mole % and free amphotericin samples by more amorphous (presumably toxic) rougher-textured material (data not shown).

To determine whether any of the ribbon structures shown in Fig. 3 were capable of occluding an aqueous volume (i.e., were liposomal), we performed captured volume measurements. Pure [Myr_2]PtdCho/[Myr_2]PtdGro systems were able to capture 7.5 μl of buffer per μmol of lipid, consistent with what has been reported for other negatively charged liposomes (14). When 5 mol % amphotericin was incorporated into these systems, however, the captured volume fell precipitously to 0.51 μl/μmol. Although it is possible that this was mostly due to vesicles made leaky by sequestered

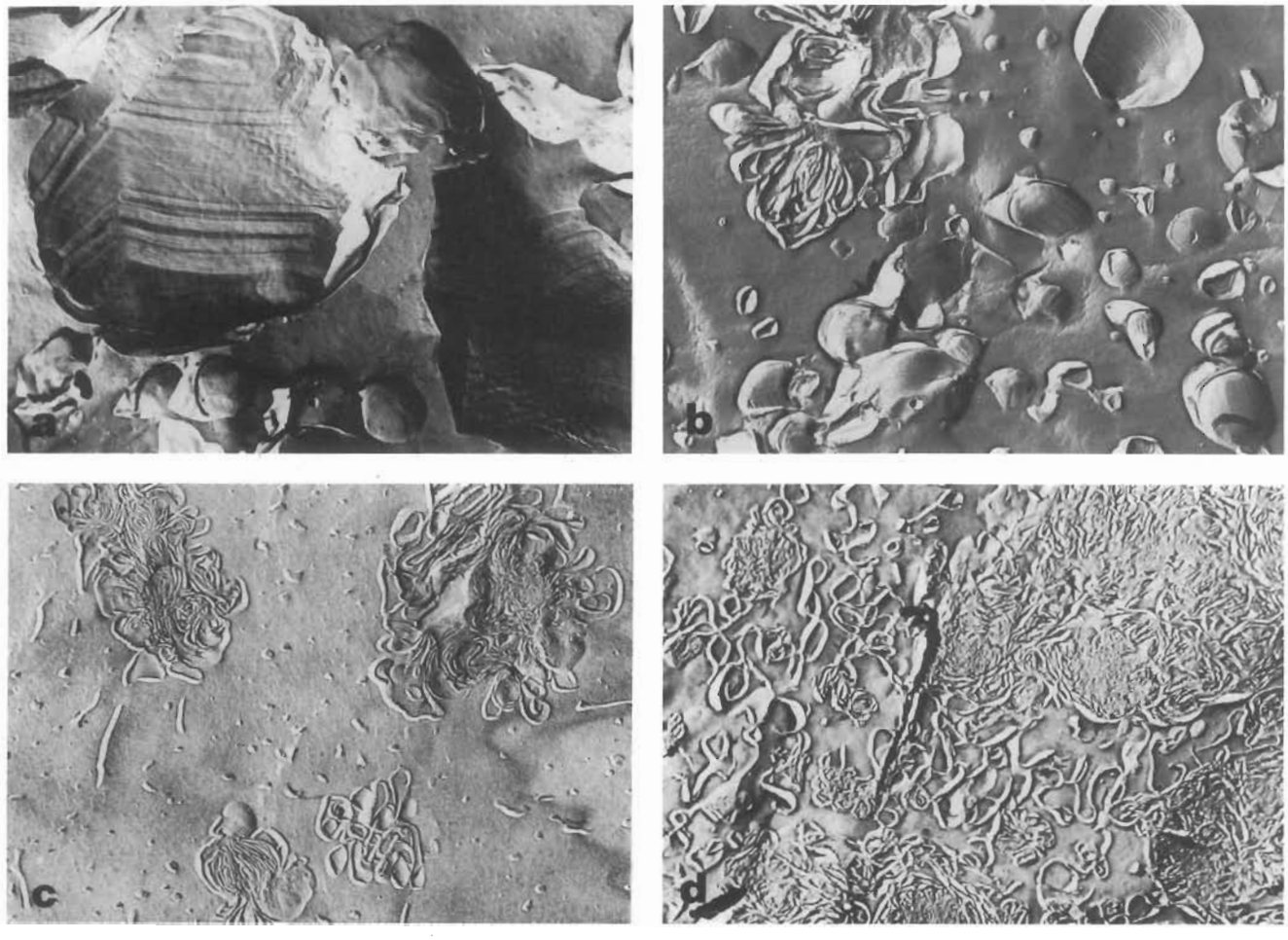

FIG. 3. Freeze–etch electron micrographs of various [Myr_2]PtdCho/[Myr_2]PtdGro/amphotericin B dispersions quenched from 20°C. All systems contained [Myr_2]PtdCho/[Myr_2]PtdGro in a molar ratio of 7:3 and an amphotericin B molar percentage (with respect to the bulk lipid) of 0% (*a*), 5% (*b*), 25% (*c*), and 50% (*d*). Samples were prepared by quick freezing into liquid propane without a cryoprotectant. Replicas were viewed on a Philips 300 electron microscope. (×25,000; 1 cm = 0.4 μm.)

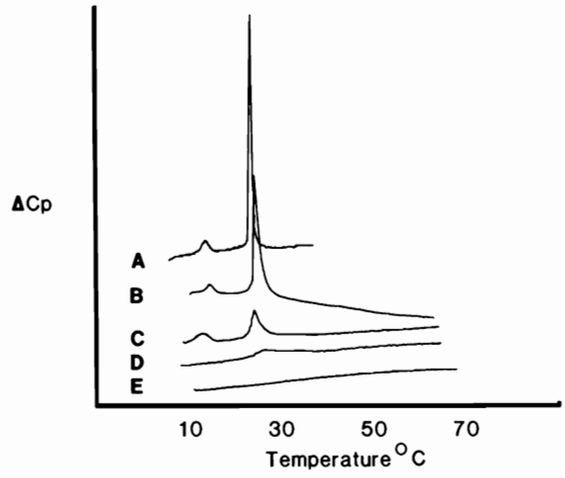

FIG. 4. Differential scanning calorimetry endotherms of [Myr_2]PtdCho/[Myr_2]PtdGro, 7:3 (mol/mol), dispersions containing 0 (trace A), 5 (trace B), 25 (trace D), and 50 (trace E) mol % amphotericin B. The 25 mol % sample was also rescanned after being held at 60°C for 0.5 hr (trace C).

amphotericin, both captured volume measurements, which suggested zero occluded volume, and freeze–etch studies were in agreement and supported the observation that the 25 and 50 mol % preparations were substantially free of vesicles. The nonvesicular nature of these preparations led us to studies aimed at uncovering the physical nature of the lipid.

Differential scanning calorimetry endotherms are shown in Fig. 4. The unperturbed [Myr_2]PtdCho/[Myr_2]PtdGro system and the system with 5 mol % of incorporated amphotericin B showed clearly definable pretransitions at 13°C and main transitions at 23–24°C. Amphotericin, at this concentration, may have broadened and elevated the main transition somewhat, consistent with a drug–lipid interaction (15). At 25 mol % amphotericin, however, there was only a very weak remnant of a transition and at 50 mol % amphotericin no transitions at all were visible.

^{31}P NMR performed on all of these samples yielded complementary data. A significant and progressive amount of line broadening was observed as the molar ratio of amphotericin increased in the bulk lipid. The effective chemical shift anisotropies were determiend to be 41 ppm for the 0 mol % sample, 67 ppm for the 5 mol % sample, 87 ppm for the 25 mol % sample, and 106 ppm for the 50 mol % sample. This would be expected to result from progressively immobilized lipid (16) and clearly suggested that the dampening of the endothermic behavior observed in the differential scanning calorimetry studies arose from phenomena other than just the destruction of the cooperative unit.

Without a doubt, wide-angle x-ray diffraction measurements provided a rich source of data in the characterization of the lipid component of these systems. Pure [Myr_2]PtdCho/[Myr_2]PtdGro, 7:3 (mol/mol), and the 5, 25, and 50 mol % amphotericin samples were studied at 20°C, 25°C, and 40°C (Fig. 5). At 20°C the pure lipid system exhibited a relatively sharp peak at ≈4.2 Å characteristic of the well-ordered side-by-side packing of the hydrocarbon chains in gel-phase lipid. When the sample temperature was raised to 25°C, this peak was replaced by a weaker diffuse band suggesting, as had the calorimetry, that a gel to liquid crystalline transition had occurred. When 5 mol % or greater amphotericin was incorporated into the bulk lipid, however, the 4.2-Å peak was evident at 20°C and 25°C signaling the persistence of gel-phase lipid. Again these results were foreshadowed by the ^{31}P NMR and differential scanning calorimetry studies that detected motionally restricted lipid in these samples. At 40°C there was no evidence of gel-phase lipid in the 0 and 5 mol % systems, but unmelted lipid was clearly present in the 25 and 50 mol % samples. Thus, the differential scanning calorimetry, ^{31}P NMR, and wide-angle x-ray diffraction data supported a model in which the amphotericin at increasing mol fractions caused a progressive trans rotational isomerization or "freezing out" of the bulk lipid.

We next turned our attention to the aggregation state of the amphotericin itself. We reasoned that as the mol fraction of lipid decreased in our preparations the amphotericin would become increasingly aggregated. Such aggregation phenomena have been detected by absorbance spectroscopy (17) and we applied these principles here. As shown in Fig. 6 (*Upper*) absorbance at longer wavelengths was attenuated as the mol fraction of amphotericin increased in the bulk lipid phase. This is consistent with increased chromophore aggregation or stacking and can be interpreted in terms of exciton splitting

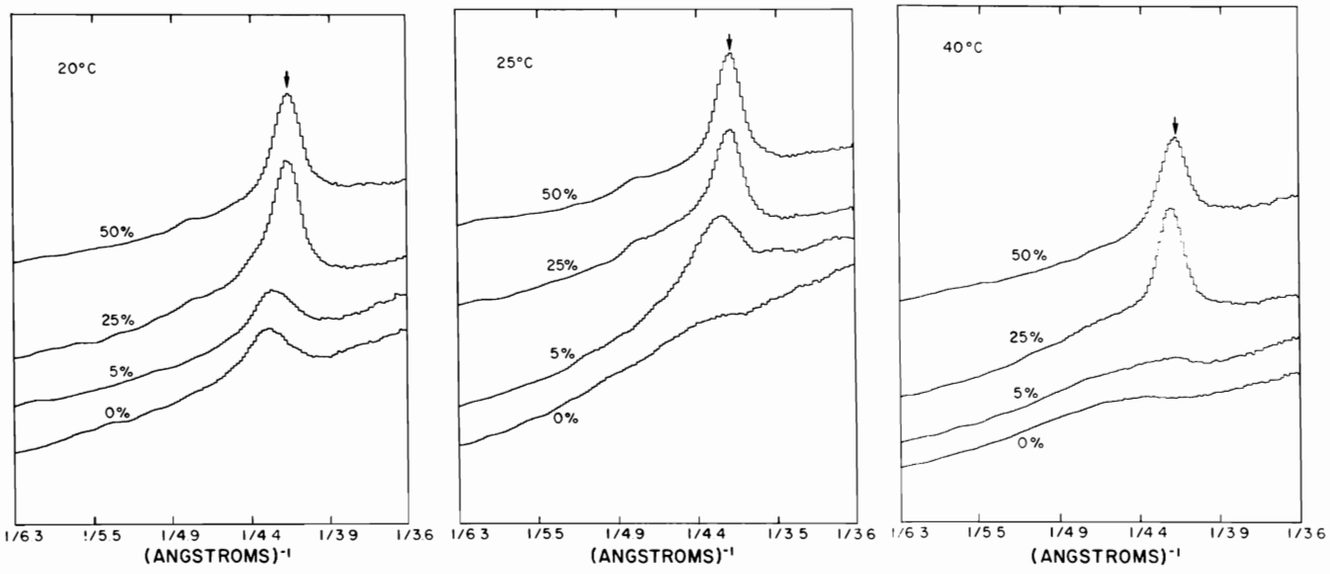

FIG. 5. Wide-angle x-ray diffraction of [Myr_2]PtdCho/[Myr_2]PtdGro, 7:3 (mol/mol), dispersions containing 0, 5, 25, or 50 mol % amphotericin B at 20°C, 25°C, and 40°C. The intensity of x-ray diffraction is shown vs. the scattering angle; zero scattering angle is off the graph to the left. The predominant feature at low temperatures and/or at high amphotericin B fractions is a peak at 4.1–4.2 Å (arrow), indicating the presence of gel-state lipid. The slow gradual rise in intensity from left to right in the samples is due to incoherent scatter.

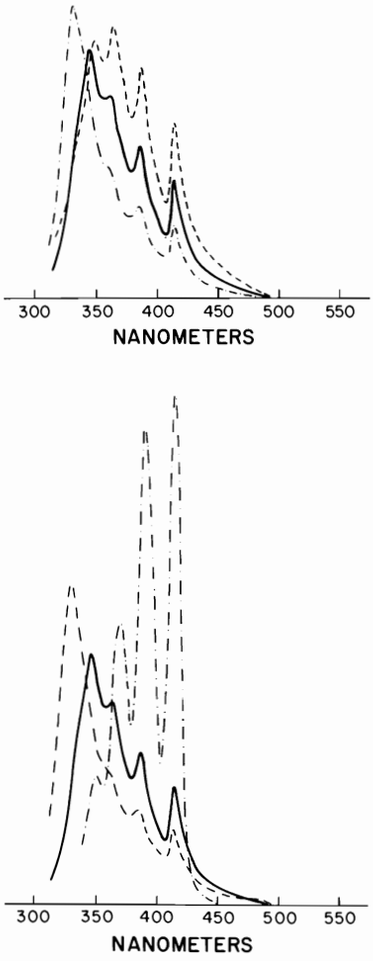

FIG. 6. (*Upper*) Absorbance spectra of [Myr_2]PtdCho/[Myr_2]PtdGro, 7:3 (mol/mol), dispersions containing 5 mol % (---), 25 mol % (——), or 50 mol % (·–·) amphotericin. Amphotericin concentration was held constant at 25 μM. Absorbances at wavelengths <350 nm were increased due to multiple scatterings. (*Lower*) The 25 mol % preparations before (——) and after (---) heating for 0.5 hr at 60°C. ·–·, superimposable spectra arising from 5, 25, and 50 mol % samples diluted 1:10 in 4% (wt/vol) deoxycholate.

(18). Fig. 6 (*Lower*) shows that when these systems were solubilized in deoxycholate, absorbance rebounded and was, in fact, equivalent in all preparations. Thus it appeared to us that in carrier systems the toxicity of the amphotericin could be related simply to its aggregation state. Clearly this aggregation was enhanced in a lipid compared to deoxycholate matrix. Moreover, in the lipid environment, the aggregation was further enhanced (with a further decrease in toxicity) when the mol fraction of amphotericin was increased.

By this hypothesis, we endeavored to manipulate the physical and toxicological properties of the 25 mol % system. Fig. 4 shows that, when this sample was heated to 60°C for 0.5 hr, a pretransition and a main transition reappeared on the calorimetric tracing, implying a phase separation of the lipid. Subsequent to this lipid phase separation an increase in amphotericin B aggregation was expected and was confirmed optically as shown in Fig. 6. Heating clearly produced a decreased absorbance consistent with an aggregation of the amphotericin chromophore as discussed above. We thus expected this heat-aggregated amphotericin system to exhibit an attenuation in toxicity, and in fact this turned out to be the case. As shown in Fig. 2, heating of the 25 mol % sample resulted in an increase in LD_{50} from between 10 and 15 mg/kg to >19 mg/kg.

The studies described here thus strongly suggest that nonliposomal-lipid-stabilized aggregates of amphotericin are responsible, at least in part, for the toxicity attenuation that has been widely reported to result from the incorporation of this drug into intact vesicles (4–7). In fact, in our hands pure [Myr_2]PtdCho and [Myr_2]PtdGro were able to promote ribbon structures and similar toxicity attenuations compared to the [Myr_2]PtdCho/[Myr_2]PtdGro, 7:3 (mol/mol), mixed system we have focused on here. Our findings are supported by earlier ^2H NMR studies that also suggest that even in low mol fraction mixtures with [Myr_2]PtdCho, amphotericin exists in an aggregated 1:1 molar complex with lipid (19). These aggregates, which are highly ordered and limit the aqueous diffusion of amphotericin (data not shown), provide a simple structural rationale for the lipid-dependent toxicity attenuation of amphotericin. This rationale offers mechanistic insights into the source of the selective toxicity of the amphotericin–lipid complex and a means, as we have shown here, for the production of less-toxic dosage forms.

We acknowledge R. Jablonski, A. Durning, and R. P. Lenk for providing formulations used in biological testing and G. Weissmann, R. Pagano, and J. Weinstein for a critical reading of the manuscript.

1. Sande, M. A. & Mandell, G. L. (1980) in *The Pharmacological Basis of Therapeutics*, eds. Gilman, A. G., Goodman, L. S. & Gilman, A. (MacMillan, New York), pp. 1233–1236.
2. DeKruijff, B., Gerritsen, W. J., Oerlemans, A., Demel, R. A. & VanDeenen, L. L. M. (1974) *Biochim. Biophys. Acta* **339**, 30–43.
3. Croquin, A. V., Bolard, J., Chabbert, M. & Gary-Bobo, C. (1983) *Biochemistry* **22**, 2939–2944.
4. New, R. R. C., Chance, M. L. & Heath, J. (1981) *Antimicrob. Chemother.* **8**, 371–381.
5. Graybill, J. R., Craven, P. C., Taylor, R. L., Williams, D. M. & Magee, W. E. (1982) *J. Infect. Dis.* **145**, 748–752.
6. Lopez-Berestein, G., Mehta, R., Hopfer, R. L., Mills, K., Kasi, L., Mehta, K., Fainstein, V., Luna, M., Hersh, E. M. & Juliano, R. L. (1983) *J. Infect. Dis.* **147**, 939–945.
7. Juliano, R. L., Grant, C. W. M., Barber, K. R. & Kalp, M. A. (1986) *Mol. Pharmacol.* **31**, 1–11.
8. Lopez-Berestein, G., Fainstein, V., Hopfer, R., Mehta, K., Sullivan, M. P., Keating, M., Rosenblum, M. G., Mehta, R., Luna, M., Hersh, E. M., Reuben, J., Juliano, R. L. & Bodey, G. P. (1985) *J. Infect. Dis.* **151**, 704–710.
9. Lopez-Berestein, G. (1987) *J. Clin. Oncol.* **5**, 310–315.
10. Szoka, F. C., Milholland, P. & Barza, M. (1987) *Antimicrob. Agents Chemother.* **31**, 421–429.
11. Mehta, R., Lopez-Berestein, G., Hopfer, R., Mills, K. & Juliano, R. (1984) *Biochim. Biophys. Acta* **770**, 220–234.
12. Reed, L. J. & Muench, H. (1938) *Am. J. Hyg.* **27**, 493–497.
13. Gruner, S. M., Lenk, R. P., Janoff, A. S. & Ostro, M. J. (1985) *Biochemistry* **24**, 2833–2842.
14. Deamer, D. W. & Uster, P. S. (1983) in *Liposomes*, ed. Ostro, M. J. (Dekker, New York), pp. 27–51.
15. Carter, B. R., Chapman, D., Hawes, S. M. & Saville, J. (1974) *Biochim. Biophys Acta* **363**, 54–64.
16. Seelig, J. (1978) *Biochim. Biophys. Acta* **515**, 105–140.
17. Sauer, R., Smith, J. R. L. & Schultz, A. J. (1966) *J. Am. Chem. Soc.* **88**, 2681–2688.
18. Kasha, M., Rawls, H. R. & El-Bayoumi, M. A. (1965) *Pure Appl. Chem.* **2**, 371–392.
19. Dufourc, E. J., Smith, I. C. P. & Jarrell, H. C. (1984) *Biochim. Biophys. Acta* **778**, 435–442.